Proceedings of the
International Conference on Mechanical and Renewable Energy 2015
(ICMERE2015) 26-29 November, 2015, Chittagong, Bangladesh

ICMERE2015-PI-250

BIMETALLIC Cu-Ni CATALYSTFOR AQUEOUS-PHASE REFORMINGOF GLYCEROL

M. M. Rahman[1*] and Andrew T. Harries[2]

[1]Department of Mechanical Engineering, Chittagong University of Engineering & Technology, Chittagong 4349, Bangladesh
[2]Laboratory for Sustainable Technology, Sydney University, Australia
[*]mmrahman.cuet@gmail.com
harries@sydneyuni.au

Abstract-*Aqueous-phase reforming of glycerol was investigated over a series of Ni and Cu–Ni bimetallic catalysts supported on multi walled carbon nanotubes (MWNT). The reaction was carried out in a continuous flow fixed bed reactor (240 ℃, 40 atm) with a solution of 1 wt% glycerol in DI water at a flow rate of 0.05mLmin^{-1}.Amongst the catalysts tested, bimetallic 1Cu–12Ni/MWNT catalyst gave the higher H_2 selectivity (86%) and glycerol conversion (84%) than the benchmark12Ni/MWNT catalyst. Irrespective of Cu and Ni ratio, bimetallic Cu-Ni catalysts showed higher selectivity and glycerol conversion towards H_2 production than the Ni catalyst. The presence of Cu in bimetallic catalysts resulted in suppression of undesirable methanation reaction. Catalysts characterized by XRD and XPS showed a significant peak shift of Ni in bimetallic Cu–Ni catalysts than the Ni catalyst, suggesting a strong interaction between Cu and Ni. Also H_2–TPR analysis showed that introducing Cu increased Ni reducibility. The bimetallic interaction is thought to be responsible for the lowered methane yield and ultimately, higher hydrogen yield observed.*

Keywords: Bimetallic catalyst, Aqueous phase reforming, Glycerol, Hydrogen

1. INTRODUCTION

Hydrogen, a clean fuel that emits only water when combusted or oxidized in PEM (proton exchange membrane) fuel cells, is in growing demand due to the technological advancements made in the fuel cell industry[1].Preferably, H_2 used for fuel should be generated from renewable sources such as solar power and biomass, rather than from fossil fuels, which are currently the primary source of H_2. A candidate source of renewable H_2 is glycerol, a byproduct of the biodiesel industry that is produced from the transesterification of vegetable oils or animal fats. The production of one ton of biodiesel also gives ~110 kg of crude glycerol (~100 kg pure glycerol)[2], and increased biodiesel production caused the price of glycerol to drop by more than half from 2003 to 2010[3]. During this same period, the aqueous-phase reforming (APR) process, pioneered by the Dumesic group in 2002[4], saw significant development. This reaction uses supported metal catalysts to generate hydrogen from oxygenated hydrocarbons in a single reactor, and is operated at higher pressure, but lower temperature, than catalytic steam reforming[5],avoiding the energetically costly vapourization of water and substrate[6]. Additionally, the lower temperatures used in APR favour the exothermic water-gas shift (WGS) reaction, allowing H_2 to be produced with minimal CO generation[6, 7]; this is crucial as CO is a known poison for Pt-based fuel-cell catalysts[6].

Supported Cu-Ni catalysts have also gained attention in APR and other systems. Though inactive for alkane hydrogenolysis[8], Cu is a highly active water-gas shift catalyst[9], making it a good potential complement to Ni. For example, the addition of Cu to a Ni catalyst for the steam reforming of ethanol reduced selectivity to CO more than it reduced selectivity to H_2, thus giving a net benefit in selectivity, and improved resistance to coke formation[10]. Additionally, adding Cu to Ni catalysts for the steam reforming of methane enhanced the WGS activity during that reaction[11]. Multiwalled carbon nanotubes (MWNTs) are useful catalyst supports as they have high surface areas on which metals can be supported, and feature interparticle mesopores that lower mass-transfer resistance. They are thermally conductive, and thermally stable at temperatures relevant to APR, even

after functionalization with Ni[12]. To date, most C-supported catalysts for APR have been based on noble metals, and few have been bimetallic.

2. EXPERIMENTAL

2.1 Catalyst Preparation

The carbon nanotubes were sonicated in 1M HNO_3 at 25 °C (Branson sonifier 450) at 20 kHz for 15 min. The objectives were to obtain good dispersion of MWNT in solution and to ensure surface modification of the outer layer of the MWNT with functional groups (i.e. –COOH and –OH) to provide nucleation sites for the deposition of Cu and Ni nanoparticles. The surface modification of MWNT is necessary for metal deposition onto carbon[13, 14]. The nanotubes were then filtered and dried for further use.CuN_2O_6 . $2.5H_2O$ (Sigma–Aldrich) and $Ni(NO_3)_2{\cdot}6H_2O$ (Stem Supply) were dissolved, individually or together, into Propylene Glycol (PG) to make monometallic or bimetallic catalysts, respectively. These were deposited on modified MWNT using reflux method. The mixture was then sonicated for 15 min. and then NaOH was added to get the mixture P^H = 9.5~10. Refluxing of the total mixture was done with the help of a oil bath at 140 °C for 2 h and at the same time the mixture was stirred with the help of magnetic stirrer. After refluxing the sample was washed couple of times to get rid of PG and to get the P^H neutral. The sample was then dried in vacuum oven at 120 °C for 12 h and calcined under flowing NO (1.5 vol.% in Ar) at 500 °C for 2 h (heating rate 10°Cmin^{-1}). Catalysts were reduced in situ in flowing H_2 (25 vol.% inAr) at 650°C for 1 h (heating rate 10°Cmin^{-1}) at atmospheric pressure.

2.3 CatalystTest

The APR of glycerol was studied in a continuous flow type fixed bed reactor system.The catalyst (150mg) was loaded into a 5-mm i.d. stainless steel tubular reactor and held in position with quartz wool plugs. Reaction temperaturewas measured by a K-type thermocouple that was placed inside the reactor, very close to the catalyst bed. The reactor was mounted in a tube furnace (MTI GSL-1100X). A backpressure regulator (0 to 1000 psig,Swagelok) attached to a pressure gauge was used to pressurize the system with Ar to 40 bar.A 1-wt% glycerol solution was introduced by a hplc digital pump (Waters 510) at a rate of 0.05 mL/min, and heating of the catalyst bed was initiated. When the reactor reached at 240°C, Ar flow was set at 50 sccm using a Bronkhorst mass flow controller. The system was allowed to stabilize for about 2 h before analysis of the reaction products began.

Gas products were analyzed at 25-min intervals using an online gas chromatograph (Varian CP-3800) equipped with one Hayesep N, 60/80 Mesh, 5 m x 1/8″ SST column and one Molsieve 5Å, 60/80 Mesh, 1 m x 1/8” column, connected in series. Liquid products were analyzed with a Shimadzu HPLC, comprising a degasser (DGU–20A5), a pump (LC–20AD), an autosampler (SIL–20A HT), an oven (CTO–20A), and a refractive index detector (RID–10A).

3. RESULTS AND DISCUSSIONS

3.1 Catalyst Characterization

Table 1: Average crystalite size and metal dispertion

Catalysts	Crystal size [15][a]	M_{disp} (%)[b]	Crystal size [15][c]
12Ni/MWNT	15.8	6.4	21.7
1Cu-12Ni/MWNT	9.8	10.3	11.3
6Cu-12Ni/MWNT	13.7	7.4	24
12Cu-12Ni/MWNT	17.8	5.7	29.4
12Cu/MWNT	21.1	4.8	–

Crystallites size and metal dispersion have shown in Table1. The addition of Cu to the Ni catalysts resulted in reduction of the crystallite size from 15.8 to 9.8 nm for 12Ni/MWNT and 1Cu–12Ni/MWNT samples, respectively. Also addition of 1 wt% Cu with 12 wt% Ni improved the Ni dispersion (Table 1). Unfortunately, higher amounts of Cu (6 and 12 wt%) did not promote further reduction in crystallite sizes of the Cu–Ni catalysts, and did not favour Ni dispersion as well. Investigation of the spent samples with XRD showed no detectable change for the 1Cu-12Ni/MWNT sample but substantial narrowing occurs for the 12Ni, 6Cu-12Ni and 12Cu-12Ni/MWNT catalysts.The average nickel crystallitesize increased from 15.8 nm to 21.7 nm and the 12Cu-12Ni crystallites increased from 17.8 nm to 29.4 nm (Table1). An increase in crystallite size from 13.7 nm to 24 nm was alsodetected for the spent 6Cu-12Ni/MWNT sample.

In order to see any interaction between Cu and Ni, the catalysts were reduced at 650 °C in flowing H_2 (25 vol.% with Ar) for 1 h (ramp rate of 10°C min^{-1}). XRD pattern of reduced catalysts have shown in Fig.1. The reduction resulted in the formation of metallic nickel (Ni^0) with diffraction peaks at 44.55, 51.84 and 76.31, corresponding to the (111), (200) and (220) planes respectively, demonstrating that activation of the catalysts were effective [16]. As we introduced Cu with 12Ni/MWNT sample, then peak shift of Ni was observed to lower diffraction angle (2θ) and the peak shift increases as the Cu loading (wt%) increases from 1 to 12 wt%. Since Cu and Ni are mutually soluble in each other for any compositions [17], thus it is possible that copper forms an alloy with nickel and this may be the explanation for the absence of diffraction peaks related to metallic copper (Cu^0) in the xCu–12Ni/MWNT samples (Fig. 1) after reduction [18].

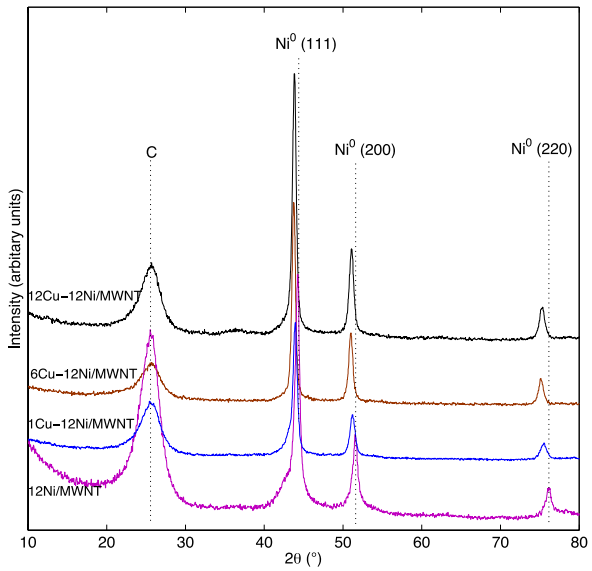

Fig. 1:X-ray diffraction patterns of 12Ni/MWNT and xCu-12Ni/MWNT catalysts. Catalysts were reduced at 650 °C in flowing H_2 (25 vol.% in Ar) for 1 h (ramp rate of 10 °C/min)

H_2-TPR profiles of the calcined catalysts have shown in Fig.2. The 12Ni/MWNT sample showed reduction peak at about 580 °C, which corresponds to the reduction of the nickel species Ni^{2+} to Ni^0. This temperature is higher than that for pure NiO, which is reduced at 300–450 °C[18], demonstrating an interaction of the nickel with the supported nanotubes. The 1Cu–12Ni and 12Cu–12Ni/MWNT catalysts showed reduction peaks at lower temperature than the 12Ni/MWNT sample but at higher temperature (420 °C, not shown in Fig.2) than the pure 12Cu/MWNT sample (Pure CuO has a reduction temperature in the range of 200 to 400 °C [19]), which indicates Cu-Ni alloy formation.

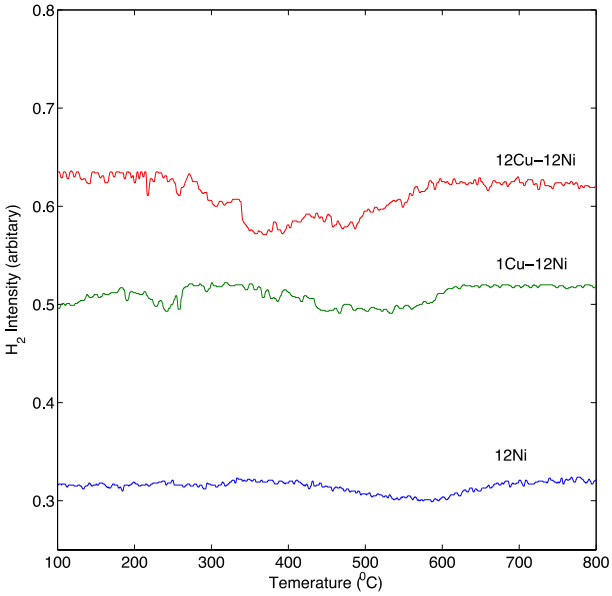

Fig.2:H2-TPR profile of the xCu-12Ni/MWNT catalysts. Analysis conditions: ~50 mg sample, 1.6% H2 in Ar, 30 sccm, heating at 10 °C/min over 100–800 °C, MS sampling at 15 scans/ min

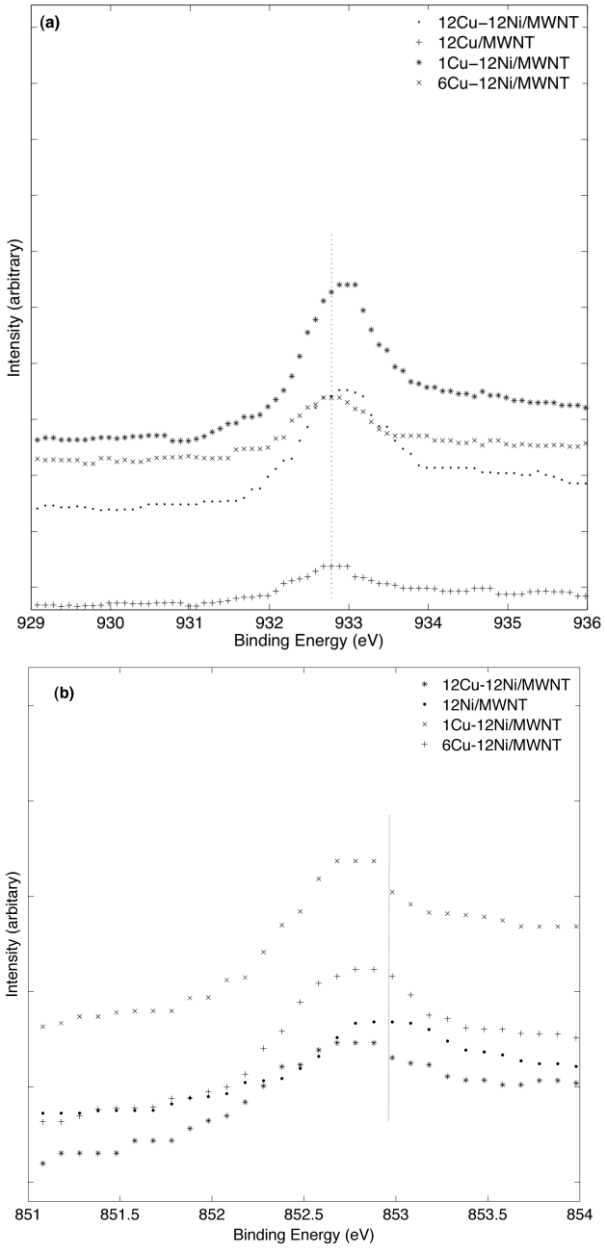

Fig.3:XPS patterns of (a) 12Cu, xCu-12Ni and (b) 12Ni, xCu-12Ni catalysts. Samples were reduced at 650 °C in flowing H2 (25 vol.% in Ar) for 1 h (ramp rate of 10 °C min-1)

As shown in Fig.3, the Cu 2*p* XPS peak (Figure 3(a)) of xCu–12Ni catalysts shifted to higher binding energy compared to pure Cu catalyst, in particular to 1Cu-12Ni sample, indicating that the electronic structure of Cu was modified when Ni was introduced. Also Ni 2*p* peak (Figure 3(b)) intensity decreases as the Cu/Ni atomic ratio increases. The xCu–12Ni peak shifted to low binding energy compared to pure 12Ni peak. This result is similar to the results of Pt coated Au nanoparticles with core-shell structure [20].

3.2 Catalytic Tests

An aqueous solution with 1 wt% glycerol was used to evaluate the performance of the catalysts. All reactions were performed at 240 °C, 40 bar, and with a feed flow

rate of 0.05 mL min^{-1}, irrespective of the catalyst used. Reaction results in terms of yield of gaseous products and H_2 selectivity are presented in Fig.4. Table 2 shows total glycerol conversion, gas phase carbon yield and system carbon balance. The reaction data presented in Figure 4 and Table 2 shows that the aqueous-phase reforming of glycerol over any of the studied catalysts indeed leads to a hydrogen-rich gas phase. Alkanes other than methane (i.e ethane and propane) were only detected for 12Ni/MWNT and 12Cu–12Ni/MWNT catalyst in trace amounts and were not further quantified.

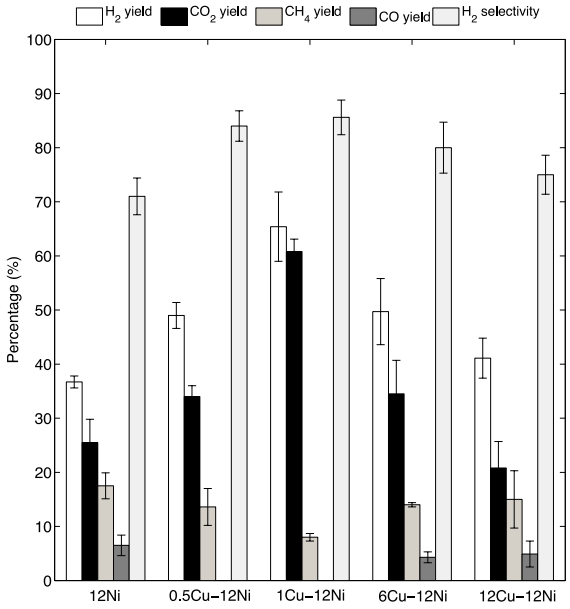

Fig.4: Effects of Cu addition to 12Ni/MWNT catalysts on yield and selectivity in the aqueous phase reforming of glycerol (240 °C, 40 bar, 0.05 mL/min, 150mg catalyst; data are mean values over t = 3–110 h). Error bars indicate one standard deviation; each bar is the average of ≥2 experiments

The H_2 yield from the APR of glycerol was calculated as the ratio of the amount of H_2 produced divided by the amount of H_2 that could have been produced if all of the glycerol was completely reformed to H_2 and CO_2 (i.e. 7 theoretical mol H_2/mol glycerol). Comparing the catalytic performance in terms of H_2 yield, all the Cu–Ni catalysts showed higher yield than Ni catalyst. Among the Cu–Ni catalysts tested, 1Cu–12Ni catalyst showed highest H_2 yield (65.5%) and as the Cu loading increased H_2 yield decreased. H_2 yields reported in the literature are much lower than this, for example: <6% at 240 °C/40 bar for 12.5% Ni, 2.5% Pt and 12.5% Ni–2.5% Pt catalysts supported on alumina [21], and 22.6% at 250 °C/35 bar for 5 wt% Cu-20 wt% Ni catalyst supported on hydrotalcite-like compounds (HTLCs) [22]. The low concentration of feed (1 wt% glycerol in DI water) and optimised low flow rate (0.05mL/min) could be responsible for our reported high H_2 yield (65.5%). The same trend was observed for CO_2 yield, the main C-containing product in the gas phase, that could be due to high water gas shift reaction favoured by Cu [23]. Cu–Ni catalysts showed lower CO yield than the Ni catalyst as Cu is one of the most active metal in WGS reaction [6]. No CO was detected for 0.5Cu-12Ni and 1Cu–12Ni catalyst, indicating that CO concentration in the product gas of these two catalysts was below the GC detection limit (i.e. [CO] ≤ 100 ppm) (Fig.4), and higher CO yield was observed for higher Cu loading (Fig.4). CH_4 formation was significant on the Ni catalyst, since Ni has high activity in methanation reaction [6], also Ni shows high activity in the cleavage of C–O bonds of oxygenated compounds [4].

Table 2: Glycerol conversion, Gas phase C yield in the aqueous-phase reforming of glycerol over MWNT supported catalysts (240 ºC, 40 bar, 0.05 mL/min, 150 mg catalyst; data are mean values over t = 3–110 h).

Catalysts	Total Gly. Conv.(%)	Gas phase C yield(%)	C Balance, out/in(%)
12Ni/MWNT	44	39	96
0.5Cu-12Ni/MWNT	60	54	103
1Cu-12Ni/MWNT	84	76	101
6Cu-12Ni/MWNT	77	47	98
12Cu-12Ni/MWNT	68	34	95

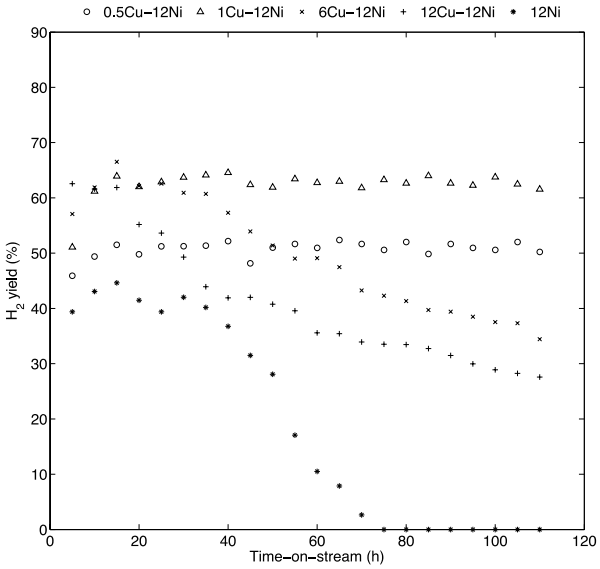

Fig.5: Variation of H_2 yield with time-on-stream in the APR of glycerol (240 °C, 40 bar, 1 wt% glycerol, 0.05 mL/min, 150 mg catalyst)

The H_2 selectivity showed the same trend as H_2 yield; Cu-Ni catalysts were more selective towards H_2 production than Ni catalyst. 1Cu–12Ni catalyst showed higher (86%) H_2 selectivity but the selectivity decreased with higher (12 wt%) Cu loading. The H_2 selectivity obtained here are quite similar with those reported by Lehnert and Claus [24] for 3 wt% Pt catalysts supported on alumina (highest H_2 selectivity obtained was 85% at 250 °C/20 bar, 10 wt% glycerol at

a flow rate of 0.5 ml min^{-1}) and Cortright et al. [4] for 3 wt% Pt catalysts supported on nanofibers of γ-alumina (highest H_2 selectivity obtained was 75% at 225 °C/29 bar, 10 wt% glycerol at a flow rate of 0.06 ml min^{-1}).

Fig.5 shows catalyst stability with time on-stream. Even though, 12Ni/MWNT, showed promising results compared to highly expensive noble metal catalyst, $3Pt/Al_2O_3$, [25] but it showed severe deactivation after 40 hours on stream, infact H_2 peak was completely disappeared after 70 h on stream (Fig.5). Also 6Cu-12Ni/MWNT and 12Cu-12Ni/MWNT catalyst showed deactivation and H_2 yield gradually decreased with time on-stream. High sintering of the active phase, as a result the particle size increased (Table 1) in relation to the fresh reduced phase could be partly responsible for their deactivation. Please note that these samples might also form a metal oxide layers on their surfaces which have diffraction lines with such low intensity that they are below the detection limit of XRD. On the other hand, no such deactivation was observed for 0.5Cu-12Ni/MWNT and 1Cu-12Ni/MWNT catalyst for 110 h on-stream. Among the bimetallic Cu-Ni catalysts we tested, 1Cu–12Ni/MWNT gave the highest H_2 yield, glycerol conversion, gas phase C yield, H_2 rate, lowest CH_4 yield and no CO concentration.

4. CONCLUSIONS

Catalyst supported on carbon nanotubes (MWNT) showed higher yield and selectivity towards hydrogen production than the oxide supports in the APR of glycerol which is related to the higher surface area, interparticle mesoporosity and higher interaction between active metal and nanotubes. Bimetallic 1Cu–12Ni/MWNT catalyst gave the higher H_2 selectivity (86%) and glycerol conversion (84%) than the bench mark 12Ni/MWNT catalyst. Irrespective of Cu and Ni ratio, bimetallic Cu–Ni catalysts showed higher selectivity and glycerol conversion. The presence of Cu (1 wt%) in bimetallic catalysts resulted in suppression of undesirable methanation reaction and enhancement of WGS reaction. The high activity and selectivity of Cu–Ni catalysts is related to the interaction between Cu and Ni, enhancement of metal dispersion and Ni reducibility.

5. REFERENCES

[1] S. Dunn, Hydrogen futures: toward a sustainable energy system, International Journal of Hydrogen Energy, 27 (2002) 235-264.

[2] A. Behr, J. Eilting, K. Irawadi, J. Leschinski, F. Lindner, Improved utilisation of renewable resources: New important derivatives of glycerol, Green Chemistry, 10 (2008) 13-30.

[3] R.L. Maglinao, B.B. He, Catalytic Thermochemical Conversion of Glycerol to Simple and Polyhydric Alcohols Using Raney Nickel Catalyst, Industrial & Engineering Chemistry Research, 50 (2011) 6028-6033.

[4] R.D. Cortright, R.R. Davda, J.A. Dumesic, Hydrogen from catalytic reforming of biomass-derived hydrocarbons in liquid water, Nature, 418 (2002) 964-967.

[5] C.H. Zhou, H. Zhao, D.S. Tong, L.M. Wu, W.H. Yu, Recent Advances in Catalytic Conversion of Glycerol, Catal. Rev., 55 (2013) 369-453.

[6] R.R. Davda, J.W. Shabaker, G.W. Huber, R.D. Cortright, J.A. Dumesic, A review of catalytic issues and process conditions for renewable hydrogen and alkanes by aqueous-phase reforming of oxygenated hydrocarbons over supported metal catalysts, Applied Catalysis B: Environmental, 56 (2005) 171-186.

[7] G.W. Huber, J.W. Shabaker, S.T. Evans, J.A. Dumesic, Aqueous-phase reforming of ethylene glycol over supported Pt and Pd bimetallic catalysts, Applied Catalysis B: Environmental, 62 (2006) 226-235.

[8] J.H. Sinfelt, Specificity in Catalytic Hydrogenolysis by Metals, in: H.P. D.D. Eley, B.W. Paul (Eds.) Advances in Catalysis, Academic Press, 1973, pp. 91-119.

[9] D.C. Grenoble, M.M. Estadt, D.F. Ollis, The chemistry and catalysis of the water gas shift reaction: 1. The kinetics over supported metal catalysts, Journal of Catalysis, 67 (1981) 90-102.

[10] A.J. Vizcaíno, A. Carrero, J.A. Calles, Hydrogen production by ethanol steam reforming over Cu–Ni supported catalysts, International Journal of Hydrogen Energy, 32 (2007) 1450-1461.

[11] T.-J. Huang, T.-C. Yu, S.-Y. Jhao, Weighting Variation of Water−Gas Shift in Steam Reforming of Methane over Supported Ni and Ni−Cu Catalysts, Industrial & Engineering Chemistry Research, 45 (2005) 150-156.

[12] M.F. Variava, T.L. Church, N. Noorbehesht, A.T. Harris, A.I. Minett, Carbon-supported gas-cleaning catalysts enable syn gas methanation at atmospheric pressure, Catal. Sci. Technol., 5 (2015) 515-524.

[13] T.W. Ebbesen, H. Hiura, M.E. Bisher, M.M.J. Treacy, J.L. Shreeve-Keyer, R.C. Haushalter, Decoration of carbon nanotubes, Advanced Materials, 8 (1996) 155-157.

[14] R. Yu, L. Chen, Q. Liu, J. Lin, K.-L. Tan, S.C. Ng, H.S.O. Chan, G.-Q. Xu, T.S.A. Hor, Platinum Deposition on Carbon Nanotubes via Chemical Modification, Chemistry of Materials, 10 (1998) 718-722.

[15] M.S. Holm, Y.J. Pagan-Torres, S. Saravanamurugan, A. Riisager, J.A. Dumesic, E. Taarning, Sn-Beta catalyzed conversion of hemicellulosic sugars, Green Chem., 14 (2012) 702-706.

[16] A. Iriondo, V.L. Barrio, J.F. Cambra, P.L. Arias, M.B. Güemez, R.M. Navarro, M.C. Sánchez-Sánchez, J.L.G. Fierro, Hydrogen Production from Glycerol Over Nickel Catalysts Supported on Al2O3 Modified by Mg, Zr, Ce or La, Topics in Catalysis, 49 (2008) 46-58.

[17] W.D. Callister, Materials science and Engineering: An introduction, John wiley & Sons, New YORK, Ch. 9, Vil. 1 (7 th edition, 2007) 184-257.

[18] L. Dussault, J.C. Dupin, C. Guimon, M. Monthioux, N. Latorre, T. Ubieto, E. Romeo, C. Royo, A. Monzón, Development of Ni–Cu–Mg–Al catalysts for the synthesis of carbon nanofibers by catalytic

decomposition of methane, Journal of Catalysis, 251 (2007) 223-232.
[19] L. Dussault, J.C. Dupin, E. Dumitriu, A. Auroux, C. Guimon, Microcalorimetry, TPR and XPS studies of acid–base properties of NiCuMgAl mixed oxides using LDHs as precursors, Thermochimica Acta, 434 (2005) 93-99.
[20] D. Zhao, B.-Q. Xu, Enhancement of Pt Utilization in Electrocatalysts by Using Gold Nanoparticles, Angewandte Chemie International Edition, 45 (2006) 4955-4959.
[21] A. Iriondo, J.F. Cambra, V.L. Barrio, M.B. Guemez, P.L. Arias, M.C. Sanchez-Sanchez, R.M. Navarro, J.L.G. Fierro, Glycerol liquid phase conversion over monometallic and bimetallic catalysts: Effect of metal, support type and reaction temperatures, Applied Catalysis B: Environmental, 106 (2011) 83-93.
[22] R.L. Manfro, T.P.M.D. Pires, N.F.P. Ribeiro, M.M.V.M. Souza, Aqueous-phase reforming of glycerol using Ni-Cu catalysts prepared from hydrotalcite-like precursors, Catalysis Science & Technology, 3 (2013) 1278-1287.
[23] M. El Doukkali, A. Iriondo, P.L. Arias, J. Requies, I. Gandarías, L. Jalowiecki-Duhamel, F. Dumeignil, A comparison of sol–gel and impregnated Pt or/and Ni based γ-alumina catalysts for bioglycerol aqueous phase reforming, Applied Catalysis B: Environmental, 125 (2012) 516-529.
[24] K. Lehnert, P. Claus, Influence of Pt particle size and support type on the aqueous-phase reforming of glycerol, Catalysis Communications, 9 (2008) 2543-2546.
[25] M.M. Rahman, T.L. Church, A.I. Minett, A.T. Harris, Effect of CeO2 Addition to Al2O3 Supports for Pt Catalysts on the Aqueous-Phase Reforming of Glycerol, ChemSusChem, 6 (2013) 1006-1013.